J-16

NUMERICAL SPECTRAL MATRIX METHOD FOR PROPAGATION IN ANISOTROPIC LAYERED MEDIA‡

Ayman A. Mostafa†, Clifford M. Krowne* and Kawthar A. Zaki†

† University of Maryland, Department of Electrical Engineering
College Park, Maryland 20742

* Code 6851, Electronics Technology Division, Naval Research Laboratory
Washington, D.C. 20375-5000.

ABSTRACT

A 6×6 macroscopic tensor is used to characterize each layer of a multilayered structure that may have arbitrary anisotropy and loss, as well as arbitrary number of conductors at each interface. The calculated propagation constant reflects the dispersion behavior of the transmission system. Numerical data are presented for both low and high anisotropy dielectric layered structures.

1. INTRODUCTION

A layered structure with some layers possessing complex anisotropy cannot be handled by a Transverse Resonance Approach (TRA) [1], or an alternate approach which specializes anisotropy to particular cases like magnetic birefringence. The transverse resonance approach, for example, is an acceptable method for isotropic layers or very simple anisotropic layers with carefully chosen principal axis orientation. A properly oriented uniaxial crystal could be analyzed by an extension of the TRA [2]. A much more powerful technique is available [3] which describes the fields by 4-element field vectors and employs a 4×4 matrix approach in the spectral domain. This matrix method can allow simultaneous permittivity, permeability, and optical activity anisotropy. Therefore, the displacement field vector can generally be described by both a permittivity tensor and an optical activity tensor. Likewise, the magnetic displacement vector can generally be described by a permeability tensor and an optical activity tensor. Now for the multilayer anisotropic structure shown in Fig. 1, each layer is characterized by a single 6×6 macroscopic tensor, which is both linear, and constant under Fourier transformed operations.

The matrix approach determines the propagation constant γ ($= -j\beta$ for lossless case) and field vectors by inverse Fourier transformation. Formulation of the numerical implementation and the numerical results generated for both low and high dielectric anisotropy layered structures are presented to demonstrate the utility of the technique.

2. FORMULATION OF NUMERICAL METHOD

For ease of calculation, the finite Fourier transform is used to transform the fields over the spatial coordinate parallel to the layer interfaces. This discrete Fourier transform is physically reasonable and convenient because the fields are confined to the region(s) of the strip lines and/or slots. The equation governing the fields in each layer is given by [3]:

$$\frac{d\tilde{\Phi}}{dy} = j\omega R\tilde{\Phi} \qquad (1)$$

where R is a 4×4 matrix and its elements are functions of ω, γ, α_n (propagation constant in x direction), permeability and permittivity as well as optical activity tensors. $\tilde{\Phi}$ is the 4-element transformed field vector containing fields tangential to the interface. Equation (1) is the state equation for the tangential field components. The solution to (1) at any point y_i' within the layer is:

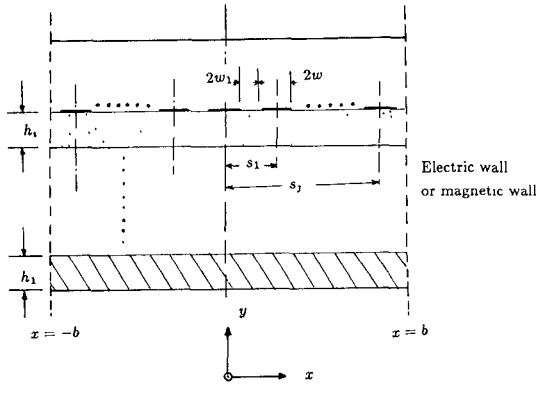

Fig. 1 Anisotropic layered media inside a shielded structure.

‡ Work supported in part by NRL Contract No. N00014-86K-2013.

0149-645X/87/0000-0311$01.00 © 1987 IEEE

$$\tilde{\Phi}(y_i') = P(y_i')\,\tilde{\Phi}(0) \quad (2)$$

where

$$P(y_i') = e^{Ay_i'} \quad (3)$$

$A = j\omega R$ and $\tilde{\Phi}(0)$ is a column vector at the interface $y_i' = 0$, i.e. the bottom of the i-th layer. The 4×4 state transition matrix P transforms the fields at $y_i' = 0$ into the field value at y_i' inside the i-th layer.

Numerical determination of P is accomplished by first finding the transverse eigenvalues k_{y_j} of A using a standard library computer routine. Next using the Cayley-Hamilton Theorem [4,5], $P(y)$ is expanded and computed as

$$P(y) = \sum_{i=0}^{3} a_i\, A^i \quad (4)$$

In general, the eigenvalues k_{y_j} may be degenerate. The coefficients a_i which are function of y can be found by solving the system of linear equation:

$$e^{k_{y_j} y} = \sum_{i=0}^{3} a_i\, k_{y_j}^i \qquad j = 1,..,4 \quad (5)$$

Eq. (5) is valid when all the eigenvalues k_{y_j} are distinct. For repeated (degenerate) eigenvalues, the derivatives of Eqn. (5) are applied [4,5].

The impedence-type Green's function is constructed by a procedure delineated in [3] yielding

$$\tilde{E}_x(n) = \tilde{G}_{11}(\gamma,n)\tilde{J}_x(n) + \tilde{G}_{12}(\gamma,n)\,\tilde{J}_z(n) \quad (6a)$$

$$\tilde{E}_z(n) = \tilde{G}_{21}(\gamma,n)\,\tilde{J}_x(n) + \tilde{G}_{22}(\gamma,n)\tilde{J}_z(n) \quad (6b)$$

where $\tilde{G}_{ij}$ is the Green's function in the Fourier transformed domain. Currents on the conducting lines are expanded in terms of a complete basis set. For fast computation trigonometric functions are used as the basis set. The current expansions used for even modes, for example, are

$$\tilde{J}_z(n) = \sum_{j=1}^{n_{ss}} \sum_{i=1}^{n_x} a_i \cos(\alpha_n s_j)\tilde{\xi}_{ei}(n) + b_i \sin(\alpha_n s_j)\tilde{\xi}_{oi}(n) \quad (7)$$

$$\tilde{J}_x(n) = \sum_{j=1}^{n_{ss}} \sum_{i=1}^{n_x} c_i \cos(\alpha_n s_j)\tilde{\eta}_{oi}(n) + d_i \sin(\alpha_n s_j)\tilde{\eta}_{ei}(n) \quad (8)$$

while for odd modes

$$\tilde{J}_z(n) = \sum_{j=1}^{n_{ss}} \sum_{i=1}^{n_x} a_i \sin(\alpha_n s_j)\tilde{\xi}_{ei}(n) + b_i \cos(\alpha_n s_j)\tilde{\xi}_{oi}(n) \quad (9)$$

$$\tilde{J}_x(n) = \sum_{j=1}^{n_{ss}} \sum_{i=1}^{n_x} c_i \cos(\alpha_n s_j)\tilde{\eta}_{ei}(n) + d_i \sin(\alpha_n s_j)\tilde{\eta}_{oi}(n) \quad (10)$$

where $n_{ss} = n_s/2, (n_s-1)/2$ for even and odd number of strips n_s respectively and n_z, n_x are the number of basis functions for $\tilde{J}_z$ and $\tilde{J}_x$. Here the spacing factor s_j is the distance from the origin to the center of the j-th strip and $\alpha_n = (2n-1)\pi/2b$, $n\pi/b$ for even and odd modes, respectively. $\tilde{\xi}_e$, $\tilde{\xi}_o$ $\tilde{\eta}_e$, $\tilde{\eta}_o$ are single microstrip even and odd basis functions of $\tilde{J}_z$ and $\tilde{J}_x$, respectively [10]. Using (7), Parseval's theorem, and a Galerkin-like approach, a determinental equation for the propagation constant can be written based on the fact that the current expansion coefficients are not a trivial null set.

3. NUMERICAL RESULTS

Numerical results are presented for single and coupled microstrip line structures which employ anisotropic sapphire substrates. These results demonstrate the matrix technique and are compared to earlier results in the literature. Since sapphire has only a moderate degree of anisotropy (about 21 percent), data is also gathered on a substrate material which has much higher anisotropy (about 40.4 percent), pyrolytic boron nitride (PBN). PBN originally stimulated interest because it had reasonable characteristic line impedance [6] for integrated circuit applications and might enable even and odd mode phase velocity differences to be reduced in coupled line structures [6-8]. Single and coupled line structures using PBN were studied in terms of material properties, predicted electrical behavior and measured performance [8].

Convergence behavior has been tested and is demonstrated in Fig. 2 by showing the variation of $\bar{\beta} = \beta/k_0$ versus spectral number n. It is seen that 70 terms is reasonable for accurate solution and fast computation. Table 1 gives $\bar{\beta}$ at three frequencies (for the parameters given in Fig. 4), for varying basis function number on each strip and shows that agreement between the $\bar{\beta}$ values is at the 4-th digit, leading us to use only the n_x, $n_z = (1,1)$ for efficient computation.

For single microstrip lines over sapphire, Fig. 3 shows the geometry and $\bar{\beta}$ versus frequency. Agreement between our results and [9] having a bilateral open structure for 2w/h = 1,2,4 cases is within 0.5% when our side wall width is ten times the substrate thickness. The parameters employed were $\epsilon_{xx} = \epsilon_{zz} = 9.4$, $\epsilon_{yy} = 11.6$, and substrate thickness 0.5 mm. Coupled microstrip over sapphire data is shown in Fig. 4. The even and odd mode dispersion curves are provided and agreement is better than 1% with [2]. The parameters used were $\epsilon_{xx} = \epsilon_{zz} = 9.4$, $\epsilon_{yy} = 11.6$, and $2w = 1.5$ mm, $2w_1 = 1.5$ mm, substrate thickness $h_1 = 1.5$ mm, $h_2 = 3$ mm, and $2b = 8.5$ mm.

PBN dispersion curves for coupled microstrip for even and odd modes up to 20 GHz are shown in Fig. 5 using the same geometric parameters as in Fig. 4 but here $\epsilon_{xx} = 5.12$, and $\epsilon_{yy} = 3.40$. Notice that the first higher order mode is even.

Table (1a) Odd Modes

	(n_x,n_z)			
F(GHz)	(1,1)	(1,2)	(2,1)	(2,2)
2	2.5177	2.5176	2.5179	2.5176
10	2.6946	2.6947	2.6947	2.6946
20	2.9927	2.9921	2.9928	2.9921

Table (1b) Even Modes

	$\tilde{\beta}$ for different (n_x,n_z)			
F(GHz)	(1,1)	(1,2)	(2,1)	(2,2)
2	2.6884	2.6883	2.6886	2.6882
10	3.0412	3.0408	3.0412	3.0406
20	3.2046	3.2031	3.2047	3.2031

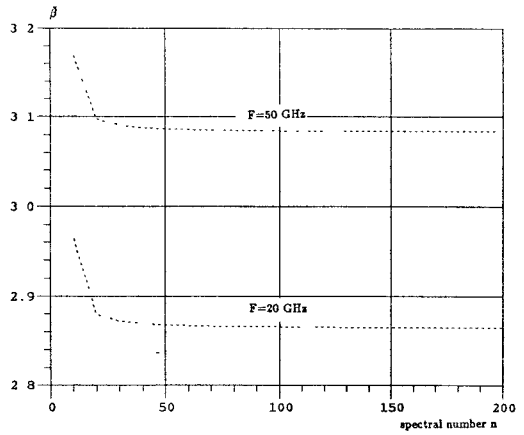

Fig.2 $\bar{\beta}$ versus spectral number n
Parameters are as in Fig. 3 with $\frac{w}{h}$=0.5

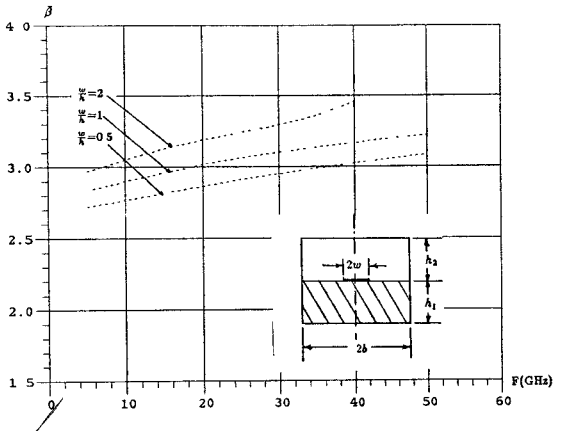

Fig. 3. Dispersion characteristics $(\bar{\beta} - \omega)$
for single microstrip strip line over saphire substrate.
$h_1 = 0.5mm$, $h_2 = 4.5mm$.

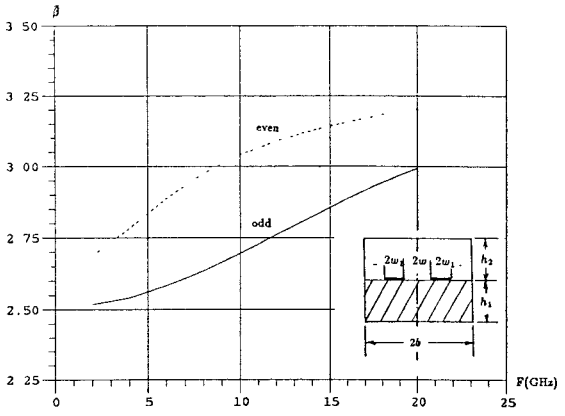

Fig. 4. Dispersion characteristics $(\bar{\beta} - \omega)$
for coupled microstrip lines over saphire substrate.
h_1 = 1.5mm, h_2 = 3mm, and $2b$ = 8.5mm.

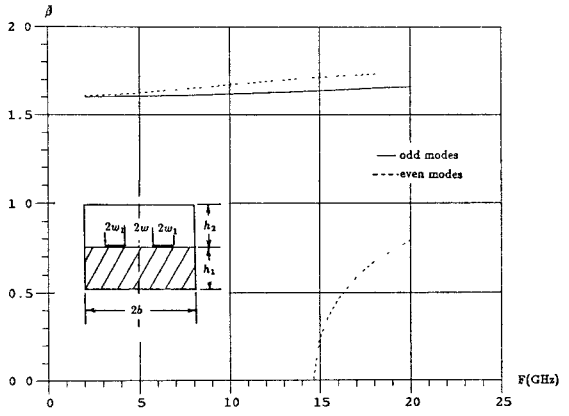

Fig. 5. Dispersion characteristics $(\bar{\beta} - \omega)$
for coupled microstrip lines over PBN substrate.
h_1 = 1.5mm, h_2 = 3mm, and $2b$ = 8.5mm.

4. CONCLUSION

Numerical implementation of a general 4×4 matrix technique to find the propagation characteristics of highly anisotropic layered media is demonestrated. The accuracy of the implementation has been checked and found to agree with previous calculations for some special cases. New results for a highly anisotropic layered structure are presented.

REFERENCES

[1] T. Itoh, "Spectral-Domain Immitance Approach for Dispersion Characteristics of Generalized Printed Transmission Lines," *IEEE Trans. Microwave Theory Tech.*, Vol. MTT-28, pp. 733-736, July 1980.

[2] T. Kitazawa and Y. Hayashi, "Coupled Slots on Anisotropic Sapphire Substrates," *IEEE Trans. Microwave Theory Tech.*, Vol. MTT-29, pp. 1035-1040, Oct. 1981.

[3] C. M. Krowne, "Fourier Transformed Matrix Method of Finding Propagation Characteristics of Complex Anisotropic Layered Media", *IEEE Trans. Microwave Theory Tech.*, Vol. MTT-32, pp. 1617-1625, Dec. 1984.

[4] T. E. Fortmann and K. L. Hitz, *An Introduction to Linear Control Systems*, New York: Marcel Dekker, Inc. 1977.

[5] N. Balabanian and T. A. Bickart, *Electrical Network Theory*, New York: Wiley, 1969.

[6] C. M. Krowne, "Microstrip Transmission Lines on Pyrolytic Boron Nitride," *Electronics Lett.*, Vol. 12, pp. 642-643, Nov. 1976.

[7] N. G. Alexopoulos and C. M. Krowne, "Characteristics of Single and Coupled Microstrip on Anisotropic Substrates," *IEEE Trans. Microwave Theory Tech.*, Vol. MTT-26, pp. 387-393, June 1978.

[8] C. M. Krowne and T. E. Washburn, "Pyrolitic Boron Nitride as a Microstrip Substrate Material," *IEEE Electrical Insulation*, Vol. EI-14, pp. 111-116, Apr. 1979.

[9] A.-M. A. El-Sherbiny, "Hybrid Mode Analysis of Microstrip Lines on Anisotropic Substates," *IEEE trans. Microwave Theory Tech.*, Vol. MTT-29, pp. 1261-1265, Dec. 1981.

[10] C. M. Krowne, "Slow Wave Propagation in Generalized Cylindrical Waveguides Loaded With a Semiconductor", *Int. J. Electronics*, Vol. 58, pp. 249-269, February 1985.